Fibers and Polymers 2019, Vol.20, No.2, 428-439
DOI 10.1007/s12221-019-8329-x

ISSN 1229-9197 (print version)
ISSN 1875-0052 (electronic version)

Elucidating the Coir Particle Filler Interaction in Epoxy Polymer Composites at Low Strain Rate

Rahul Kumar and Sumit Bhowmik*

Department of Mechanical Engineering, National Institute of Technology, Silchar 788010, India
(Received April 24, 2018; Revised October 2, 2018; Accepted November 12, 2018)

Abstract: Addressing the growing environmental issues and diverse range of applications, the present work is focused on the development of high potential 'agro-waste' such as 'coir filler' reinforced epoxy composite and evaluation of its critical mechanical properties under diverse constraints. The produced composite material is subjected to a tensile test with variable strain rate, fracture test, impact test and thermogravimetric analysis to assess its applicability in diverse loading and temperature environment. The experimental results display the complementary effect of coir fillers in improving the mechanical properties of the composite by two to four times as compared to neat epoxy and other bio-fibre/filler based composite materials. The increased tensile and flexural strength with filler addition confirms the evident interaction and load transfer capability of infused coir particle fillers in the epoxy matrix. The rate of crack initiation and propagation in the tensile test seems to be extremely affected by the strain rate variation and at higher crosshead speed, the fracture initiated early due to the singularity existed at the crack tip. The highest value of tensile stress and Young's modulus for the developed composite material is observed at the crosshead speed of 2 mm/min. The fracture properties is observed to be maximum for 5 wt. % filler loading and the principal mechanism of fracture failure is crack pinning. This study will be able to open new insights and establish the probable application of the low-cost agro-byproduct in the engineered value added bio-based composite material.

Keywords: Agro-waste, Coir fillers, Tensile strength, Strain rate, Fracture properties

Introduction

The fundamental aspect of sustainable growth lies in the development of the materials that overcome the challenging environmental concerns and balances the industrial carbon-dioxide (CO_2) emission at the end of their life-cycle, thus reduced global warming and improved ecological preservation [1,2]. Considering in a specified way, biodegradable natural fibrous feedstock derived from renewable resources might become the prevailing alternative for the production of relevant environment-friendly materials. These materials have a potential for the competent substitute of petroleum-based composite products and presently gained significant attention from automotive industries as they offer substantial weight savings at the same time ease of removal [3,4]. The lignocellulosic based natural fibres like kenaf, flax, jute, sisal, coir and so on have extensively been studied in their fibrous form for a diverse range of thermoplastic and thermoset composite material application [5-9]. Among the aforementioned bio-fibres, coconut coir is a versatile lignocellulosic biomass owing to its excellent weathering and abrasion resistance properties as well as low decomposition rate [10]. In addition to above, coir fibres are derived from the outer husk tissues of the fruit of coconut palm (Cocos nucifera), that established it as agriculture residues therefore easy to get at lower cost. The utilization of this agro-byproduct as a source of reinforcement in polymers will not only add the industrial values to this specific crop but also generate revenues for farming communities. The value addition to potential agriculture residues like coconut husks might be lead to the opening of an industrial door for farming communities as well as technical responsiveness for the environmental and ecological concerns.

Extensive research works have been carried out on the utilization of coconut coir as fibre reinforcement [11-13], shell particle filler reinforcement [14] and also in the making of geo-textiles for soil conservation and removing the dyes from aqueous solution [15,16]. The coir fillers exploited in the development of polymer composites are mainly derived from coconut shells by crushing and grinding the waste shell part of coconut fruits [17]. Nonetheless, the outer husk of the coconut fruits might become the potential resource for filler materials, which can be incorporated in different polymeric resins for manufacturing of suitable products applicable in automobiles and other surface transport mediums. In recent times, filler particles became the locus of research work around the world for the reinforcement in petroleum as well as bio-based polymers. The fillers in micro-scale size range are currently incorporated in polymeric matrices to tailor make the various resin properties like strength and stiffness. The functional properties of filler reinforced composites depend on the filler shape, size and extent of its dispersion in the continuous phase. Different research works on the utilization of micro-sized particle fillers as reinforcement material in the polymer matrices has been reported and enhancement in the mechanical properties of neat polymer samples was revealed [18,19]. Recently, a polylactic acid

*Corresponding author: bhowmiksumit04@yahoo.co.in

(PLA) based bio-char particle filler reinforced composite material demonstrated its highest strength and good dispersibility for the particle size range of 20-75 μm [20].

Considering the backdrop of the discussed specifics, present research work is focused to manufacture a mechanically competent polymer composite material with the combination of natural lignocellulosic agriculture by-product 'coir filler' as reinforcement and epoxy as the matrix material. The coir filler is designated as reinforcement material on account of its availability as agriculture waste, weathering resistance and cellulose content [21]. The thermoset 'epoxy polymeric resin' is selected as material matrix system owing to its good mechanical properties, uncomplicated processing and dimensional stability after curing [22]. The composite samples are prepared for five different filler wt. % viz. 2.5 %, 5 %, 7.5 %, 10 % and 12.5 % along with neat epoxy samples. The prepared material is subjected to the tensile test with variable crosshead speed to find strain rate effect on strength and modulus. The crack initiation and fracture of composite samples in uniaxial tension loading condition are explained considering the effect of strain rate for in-depth understanding of fracture mechanism. The flexural test and impact test has also been carried out to evaluate respective composite properties. The differential thermal analysis (DTA) and thermal gravimetric analysis (TGA) are conducted to study the various insights of thermal degradation of the coir-epoxy composite material. In addition to above, the morphology of composite sample is observed under scanning electron microscope (SEM) to assess filler distribution and filler-matrix interaction.

Experimental

Materials

The matrix and reinforcement materials for the present work are thermoset epoxy resin and coconut coir particle fillers respectively. The standard epoxy adhesive based resin, AW106 and hardener, HV953IN constitutes two-part matrix system, having the mixed viscosity of 45000 cP and pot life of 2 h at 25 ^{o}C. The resin and hardener system are procured from the Huntsman India. The chemical composition of the supplied resin and hardener system is Bisphenol F-epoxy resin and 1,8-p-menthanediamine respectively. The number average molecular weight of the corresponding epoxy resin lies between 700 and 1100. The specific gravity of hardener and resin are 0.92 and 1.17 g/cc respectively. The epoxy adhesive based resin is selected owing to its high viscosity, good mechanical properties and excellent dimensional stability. Other desirable properties of the chosen resin are good thermal stability and negligible

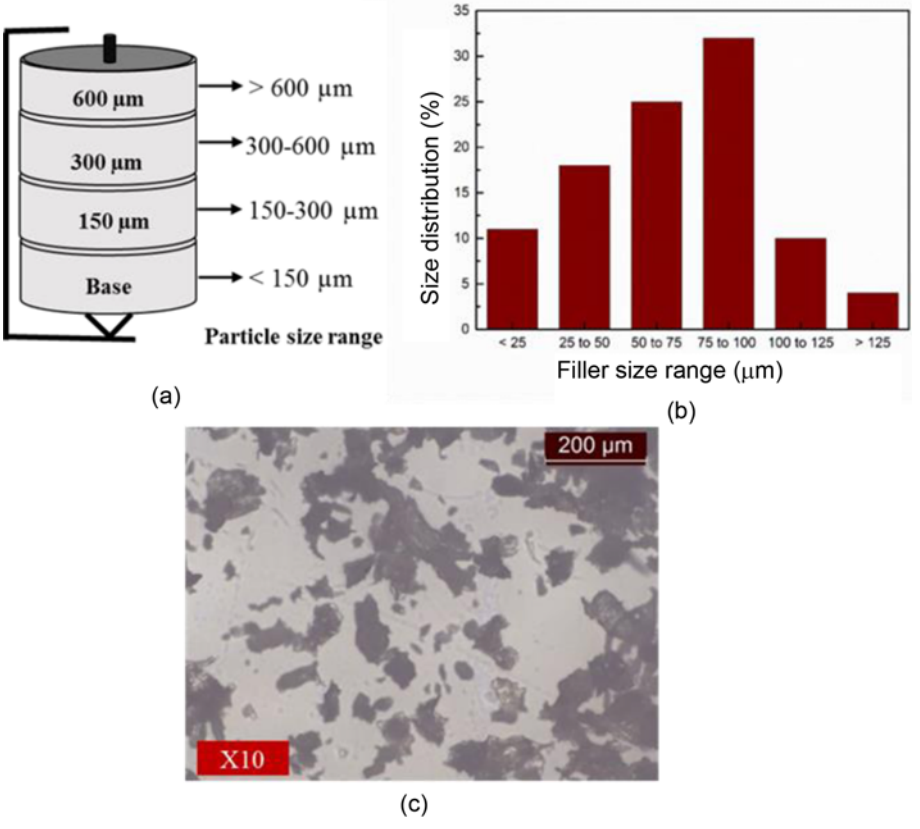

Figure 1. (a) Stacking of sieves (b) filler size distribution, and (c) optical micrograph of filler.

dimensional shrinkage on curing [23]. The high viscosity and reasonable pot life will impart better dispersibility of particle fillers and inhibit the fillers from dropping and forming agglomerates in the bottom part of resin before curing took place [24].

Filler Preparation

The main chemical constituents of coconut coir are cellulose, hemicellulose and lignin. The cellulose part gives structural strength to the fibre whereas hemicellulose provides ordinary strength as well as enables moisture absorption. The lignin part acts as a binding material for cellulose and hemicellulose along with resistance against microbial attack [25]. The reinforcing coir fillers are prepared from the outer husk of coconut fruits through mechanical processing like peeling out, breaking and grinding. The coconut coir husk is collected from the northeastern part of Indian Subcontinent. Initially the husk of the coconut was broken mechanically and then dehydrated in a hot air oven at 70 ^{o}C for 24 hours. Afterwards, the dried outer husk is pulverized into powder form first by means of a grinder used in food processing industry and then in a planetary ball mill [26]. Later on, the powdered coir particle filler is screened unto a set of sieves placed in descending order of refinement to get the complete classification of the particles below 150 μm. Consequently, the fillers are subjected to washing with acetone and distilled water subsequently to drying at 70 ^{o}C for overnight. The stacking of sieves, filler size distribution and optical micrograph for the prepared coir filler are presented in Figure 1(a), (b) and (c) respectively. The reason for choosing the particle fillers of size is their ability to disperse evenly in the matrix system along with better mechanical properties of composite [20].

Composite Preparation

The manufacturing of composite samples is initiated using glass mould of prerequisite shape and size of specimens as per respective ASTM standards. The glass mould is pre-coated with the transparent sheet and smeared with releasing agent 'silicon oil' for the easy removal of samples. The epoxy resin AW 106 and equivalent hardener HV 953IN are blended in a recommended ratio of 10:8 and stirred uniformly. Afterwards, the coconut particle filler is added to that mixture in a container and stirred for 15-17 min in an overhead mechanical stirrer and slowly discharged into the placed vacuum glass mould [27]. The whole set up with composite blends is left at room temperature for 12 h until the curing completed [28]. After that, the samples are post-cured at 70 ^{o}C for 2 h in the hot air oven and then composite specimens are used to study the various mechanical behaviour.

Testing and Characterization

Mechanical Test

The tensile, flexural, fracture and impact properties of the coir-epoxy composites are evaluated according to respective ASTM standard (with RT- 22 ^{o}C and RH- 56 %) to gauge the improvement derived from the addition of fillers.

The uniaxial tensile test is accomplished as per ASTM D 638 type V with dumbbell shape specimen of size 63.5 mm× 10 mm×3.2 mm and a gauge length of 7.65 mm. The tensile test has been carried out at three different crosshead movement (or tensile testing) speed of 1, 2 and 3 mm/min to study the strain rate effect on tensile properties. Such characterization would be highly useful to understand their appropriateness for dynamic applications in terms of varying crosshead speed. The crosshead speed can be converted into the corresponding strain rate by dividing it with gauge length of the tensile specimen.

The flexural and impact tests are conducted in accordance with ASTM D 790-03 and ASTM D 256 with specimen dimension of 65 mm×12.7 mm×3.2 mm and 63.5 mm× 12.7 mm×3.2 mm respectively. The support span of 50 mm is used in three-point bending mode of flexural test at the crosshead speed of 1.3 mm/min. The notch depth of samples in the Izod impact test is 2.54 mm.

The fracture toughness test of single edge notch bend (SENB) composite specimen are carried out as per ASTM D 5045 with specimen dimension of 55 mm×12.5 mm×6.25 mm at the crosshead speed of 10 mm/min. The values representing the Mode I fracture toughness (K_{Ic}) and fracture energy (G_{Ic}) are taken an average from the result of testing three samples from different lots.

Thermo-gravimetric Analysis

The thermogravimetric analysis is carried out using the thermal analyzer NETZSCH STA 449 F3 Jupiter. All measurements are performed from room temperature to 700 ^{o}C at a heating rate of 10 ^{o}C/min with initial sample mass of 10 mg under the nitrogen atmosphere.

Scanning Electron Microscopy (SEM)

The SEM images of coir-epoxy composite samples have been taken to examine the morphology and adhesion between the filler-matrix interfaces through electron microscope JSM-6701F. The micrographs of perpendicularly viewed samples are taken at 10 kV of the power supply with the samples layered with gold to evade charging under the electron beam.

Results and Discussion

Mechanical Properties

Tensile Properties

The mechanical properties of epoxy-based composite material reinforced with coir filler are evaluated in the uniaxial tension mode. The corresponding variation of ultimate tensile strength and elastic modulus for different filler wt. % samples combined with the neat epoxy sample are shown in Figure 2(a), (b) and (c) respectively for 1, 2 and 3 mm/min of crosshead speed. The crosshead speeds are

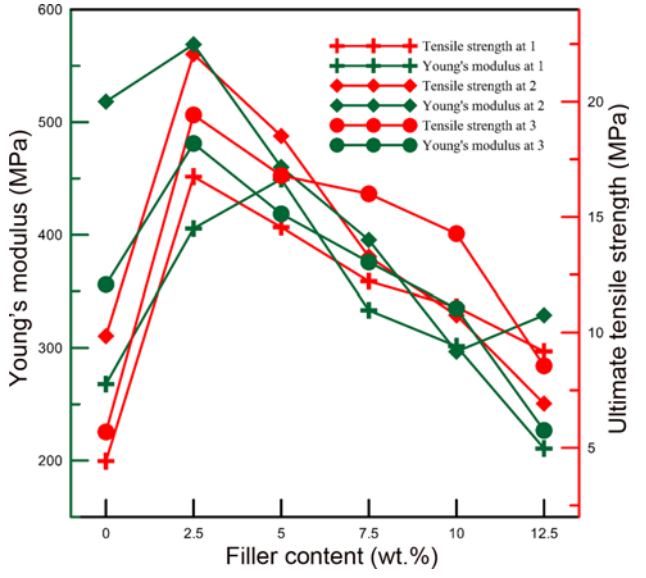

Figure 2. Tensile properties vs. filler content at different crosshead speed.

varied to study its consequence on tensile strength and Young's modulus which can identify its budding application like consumer products, building and construction uses such as decking, fencing and lineal windows or doors. Moreover, such characterization would be highly useful to understand their appropriateness for dynamic applications [29].

The neat epoxy sample has Young's modulus and tensile strength value of 518 MPa and 10 MPa respectively at 2 mm/min. The positive outcome owing to the coir filler inclusion for 2.5 wt. % of filler loading is reflected as the strength and modulus values are improved by 120 % (to 22 MPa) and 10 % (to 569 MPa) as compared to the neat epoxy material. The positive fallouts of filler addition vary from two times to three times in ultimate tensile strength values for 12.5 % and 5 % of filler content specimens as compared to neat epoxy samples at speed of 1 mm/min. This indicates the ability of coir filler to act as better reinforcement for the epoxy resin. This might be due to the enhanced load transfer capacity with the presence and distribution of particle fillers [30,31]. However, in the elastic modulus values, the improvement quantity lies from 13 % to 68 % for different filler content samples. Moreover, Young's modulus values found to be lower than the same for neat polymer for 12.5 % of filler content at 1 mm/min of crosshead speed. Nevertheless, amongst the composite samples, further inclusion of coir filler particles beyond 2.5 wt. % caused a deterioration in tensile strength and modulus of the composite material. The reason for this anticipated performance might be connected to uneven dispersion of fillers in the matrix, triggering the deprived load transfer from matrix to filler and vice-versa through the filler-matrix interface [32]. Also at higher filler weight %, the matrix material is unable to accommodate the added particle fillers, resulting in the pile up and agglomeration of fillers at several places, thus reducing the effective surface area through which stress transfer takes place. In addition to above, this may be due to the representation of the filler defects and stress concentrators [33]. Earlier research works also demonstrated the similar trends in tensile properties increment and subsequent downfall of properties at higher filler loadings [34,35].

The increase in crosshead speed is found to be substantially affected the tensile properties of the composite material. As the crosshead movement speed increases from 1 mm/min to 2 mm/min, the tensile strength of 2.5 filler wt. % samples are found to be enhanced by 32 % and corresponding modulus value is improved by 40 % for same filler loading. Quite a similar improvement in strength and elastic modulus values are demonstrated for 5 and 7.5 wt. % of coir filler samples. The triggering reason associated with this enhancement might be the orientation strengthening of filler particles at a higher speed which resulted in stretched interface area for load transfer [36]. However, at greater filler loading like 10 % and 12.5 %, significant deterioration in tensile strength of composite samples is found as speed changes from 1 mm/min to 2 mm/min. This unexpected variation may be attributed to the diminished effective interface area through which stress transfer occurs. Conversely, the additional intensification in crosshead speed to 3 mm/min prompted the anticipated drop in strength and modulus values. Especially, the fall in ultimate tensile strength value for coir filler loading of 5 wt. % is 10 % whereas the drop in Young's modulus is also 9.88 % as the speed enhanced from 2 to 3 mm/min. The highest values of tensile strength and elastic modulus are 22 MPa and 569 MPa and both are observed for 2.5 wt. % samples at 2 mm/min. The associated cause for this conduct might be the increased rate of fracture instigation and propagation at higher loading rate, thus ensuing lower breaking stress. Moreover, for filler content of 7.5 % and beyond this trend of reduction in tensile properties is reversed and an incremental variation in strength and modulus was observed. Such a performance of high filler content samples is due to the presence of high concentration of coir fillers, acting as constraints that suppress and delays the crack front formation and its proliferation. These findings have revealed the triviality of loading rate at higher filler content and prove the significance of load transferability of coir fillers at higher strain rate. Furthermore, this result indicates the more brittleness characteristics of coir-epoxy composite material at higher cross-head speed.

The fracture initiation and its growth has been observed to be substantially affected with the increase in strain rate. Taking into consideration of aforementioned results, the load required to initiate and propagate the crack is more as crosshead speed increased from 1 mm/min to 2 mm/min obtained from load-displacement curve. The higher filler content leads to an inability of epoxy resin to reach each and

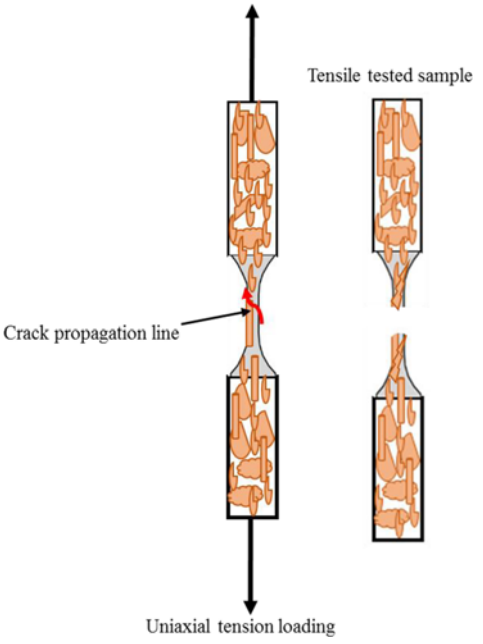

Figure 3. Tensile fracture analysis of coir filler reinforced composite sample.

every part of fillers, resulting in the formation and existence of micro cracks which acts as crack nucleation point. Also the different particle size can act as localized stress generators, initiating structural heterogeneities and resulting failure of material. The crack propagation line and obstructions confronted by the crack tip due to the presence of filler particles can be observed from Figure 3.

The filler-filler and filler-epoxy network make significant contribution to prevent the crack advancement once initiated. At high crosshead speed, these networks tend to stretch a bit more and in turn enhanced the load transferability through interphase boundary. The crack tip originated from the narrow part of the specimen and propagated through the matrix phase until the filler particles encountered to its tip. It is observed that the presence of micro size particle fillers inhibited the crack growth at higher strain rate. The scanning electron micrographs of tensile fracture surface for coir-epoxy composite samples are presented in Figure 4. The coir filler breakage after uniaxial tensile loading can be evidently observed from the presented micrograph.

The tensile properties of this developed composite material have been compared with existing different epoxy based polymer composites (presented in Table 1). The worth noting point from the presented contrast is comparable tensile strength than most of the reported works. However contrary to what was expected, the elastic modulus value shows an adversely inferior performance of the composite as compared to earlier works [37,38]. Additionally with respect to coir shell filler reinforced polypropylene and treated coir filler epoxy composite and, the difference between observed and reported values of strength (being 10 % and 27 %) are much significant, showing the latent abilities of filler reinforcement.

Flexural Properties

The flexural strength and flexural modulus at the crosshead

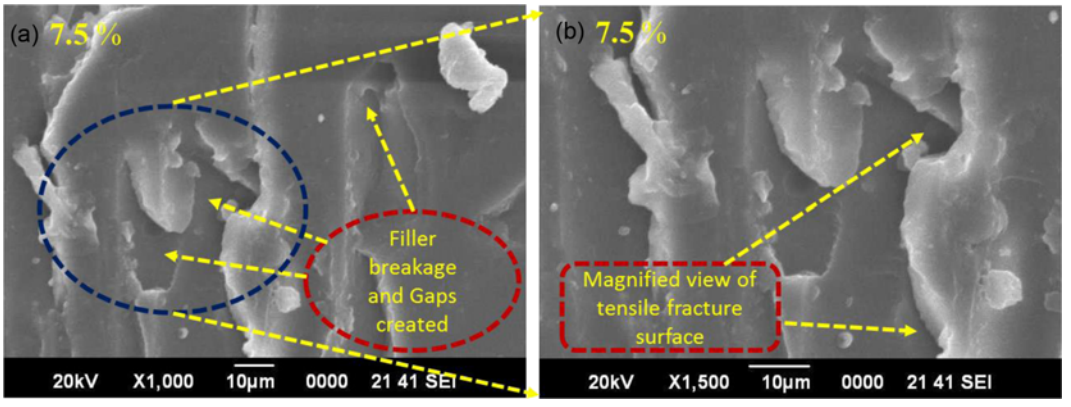

Figure 4. SEM images of tensile fracture surface of coir-epoxy composite sample.

Table 1. Comparison of tensile properties with existing coir filler based epoxy composites

Materials	Ultimate tensile strength (MPa)	Young's modulus (GPa)	Reference
Coir shell filler epoxy composite	37.30	0.688	[14]
Treated coir filler epoxy composite	28	0.739	[41]
Coir fibre epoxy composite	13.05	2.064	[50]
Present composite material	22.06	0.569	

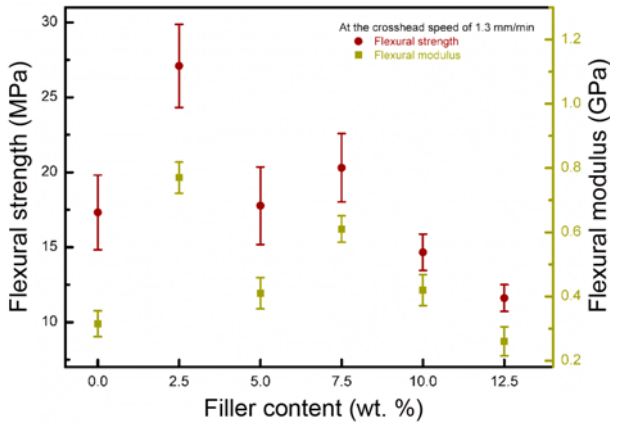

Figure 5. Flexural properties vs. filler content.

speed of 1.3 mm/min and at the strain limit 5 % for coir filler reinforced epoxy specimens along with pure epoxy samples are presented in Figure 5 where the maximum and minimum values denoted by error bars. The standard deviation for each case is also incorporated as maximum and minimum values in the diagram.

Like tensile properties, the incorporation of coir filler in the epoxy matrix caused the similar improvement in flexural strength and flexural modulus values for 2.5 wt. % of filler content. The quantitative increase in strength and modulus values as compared to the neat epoxy samples are 16 % and 23 % respectively at this filler content. The reason associated with this enhancement in flexural properties might be the improved ability to resist applied load owing to the improved interaction between matrix to filler and vice-versa through the interface with filler addition [20]. Further incorporation of coir particle fillers consequences in the downfall of flexural properties but values observed are still higher than the same for neat polymer samples. The root cause connected with the drop in properties at higher filler content is the inefficiency of stress transfer through the interface. At higher filler loading, the concentration of filler particles increases, resulting engulfing of resin and agglomeration of fillers at most of the places inside the composite samples. This is followed by reduced effective interface area of the filler-matrix interface, thus fall in flexural properties. A distinct variation in flexural properties of the composite specimen from 5-7.5 % might be due to the instrument noise and vibrations. Further addition of coir fillers beyond 7.5 % has led to the expected drop in flexural properties. The maximum value of flexural strength and modulus for the coir-epoxy composite material are 27 MPa and 0.8 GPa respectively at 2.5 wt. % of filler content. The extent of the drop in flexural properties at greater filler content is not quite similar to the same in case of tensile properties. The disparity might arise due to the fact that the three-point bending mode constitutes two different loading behaviour such as compression at top layer and tension in the bottom part.

Furthermore, the observed flexural properties of the developed material have been compared with the existing natural fibre/filler reinforced epoxy composite as presented in Table 2. The properties are found to be comparable (but lesser for most of the case) with existing various reinforced plastic materials [13,39-41]. With respect to treated coir filler based composite material, the present composite performs inferior (by about 20 %) and that might be due to the surface treatment in the former case. Concerning coir fibre based composites, the present material performs fairly better in bending load as compared to tension loading, therefore highlighting filler competitiveness.

Fracture Properties

The variation of fracture toughness and fracture energy as

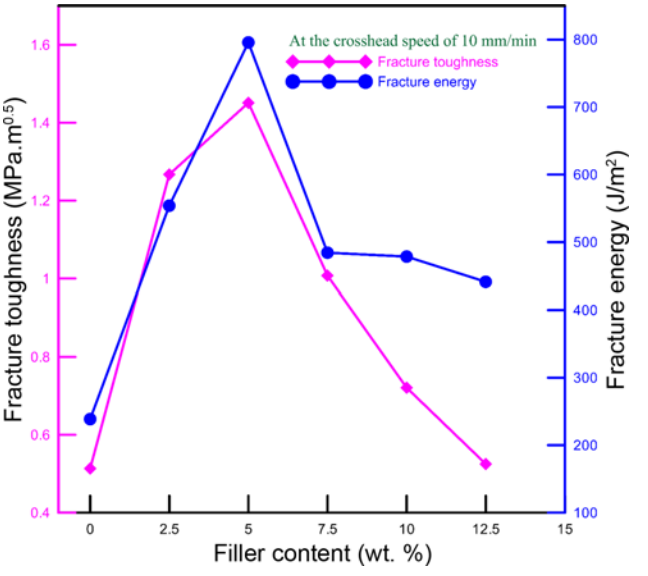

Figure 6. Fracture properties vs. filler content.

Table 2. Comparison of flexural properties with existing coir filler based epoxy composites

Materials	Flexural strength (MPa)	Flexural modulus (GPa)	Reference
Coir shell filler epoxy composite	80.68	-	[23]
Treated coir filler epoxy composite	33.88	0.79	[41]
Coir fibre-epoxy composite	35.42	-	[50]
Present composite material	27.10	0.77	

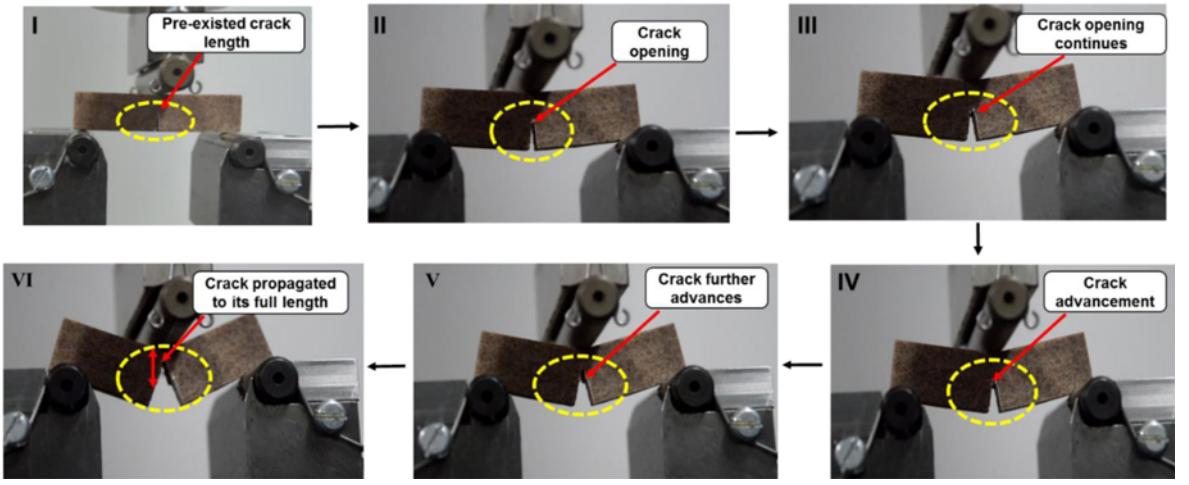

Figure 7. Different stages of crack tip propagation until fracture failure of SENB loaded specimen.

a function of filler content for composite samples along with neat epoxy specimen is depicted in Figure 6. The continuum fracture mechanics criterion states that the failure of single edge notch bend (SENB) specimen occurs when the maximum value of stress intensity factor (K) exceeds the critical stress intensity factor (K_{Ic}) also known as fracture toughness [42].

It is clearly evident that the toughness values are increased by 15 % as filler loading went up from 2.5 wt. % to 5 wt. %. Also the toughness value is found to be significantly higher than the reference neat epoxy material. The reason for this is the larger strain at the crack tip and slowing crack propagation speed in the presence of coir particles. The coir particles are remarkably stiff and resilient along the in-plane directions [34]. The obstructions to crack front propagation is resulted in the bowing of crack front between the rigid particles. This leads to secondary crack formation and in due course the improved fracture toughness value. Also the coir particle fillers played an effective role in hindering the crack initiation and propagation. The highest value of fracture toughness and fracture energy value is 1.451 $MPa \cdot m^{0.5}$ and 796 J/m^2 respectively and these values are observed for 5 wt. % of filler content. Moreover, the fracture toughness and energy values decreased with further inclusion of coir fillers and this drop continues to happen till 12.5 wt. % of filler content. Furthermore as filler loading is increased from 0 wt. % to 5 wt. %, the K_{Ic} value is enhanced by 182 % but after this as filler content varies from 5 % to 12.5 %, resulting drop in toughness value is 64 %. It seems that for better fracture properties, lower filler loading will make significant improvement as compared to virgin epoxy samples. Similarly the drop in G_{Ic} value after 5 wt. % filler content is around 45 %. However the lowest observed values for K_{Ic} and G_{Ic} are still higher than the same for neat epoxy samples. It can be noted that the 5 wt. % of filler loading is optimum with fracture properties viewpoint and any further addition in filler content cannot and will not improve the K_{Ic} and G_{Ic} values. The reason attributed to this behaviour is the severe load transferability and non-adherence of coir filler to the epoxy matrix at higher filler loading [43]. In addition, at greater filler content, the epoxy matrix would not be able reach all spaces of filler particles resulting in creation of micro-voids that acts as a designed space for crack nucleation and rapid growth. In general the load required to initiate and propagate the crack is higher in case of filler reinforced samples which offers crack bridging between two different phases that is instrumental in improving toughness value [44]. The different stages of crack propagation under the SENB loaded specimen are depicted in Figure 7 until the fracture failure occurs. The cracks initiated at the notch tip and propagated through the material traversing different pores and voids present there. Therefore the pre-existed crack is started to grow at relatively lower value of critical stress intensity factor.

Impact Properties

The ability of the material to absorb shock and energy as well as to withstand the propagation of crack is known as the impact strength. The fibre and matrix strength as well as load transfer efficiency and resistance to crack propagation play a crucial role in the evaluation of impact properties. The variation of impact resistance and breaking energy of coir filler reinforced epoxy composite in conjunction with virgin polymer samples are represented in Figure 8 where error bars signify the maximum and minimum values of respective properties.

It can be observed from the depicted variation, the composite samples have shown the increased impact resistance and breaking energy after the incorporation of coir filler in the epoxy matrix. This might be due to the inclusion of particle fillers creates an obstacle in the crack propagation. The increase in the breaking energy for different composite

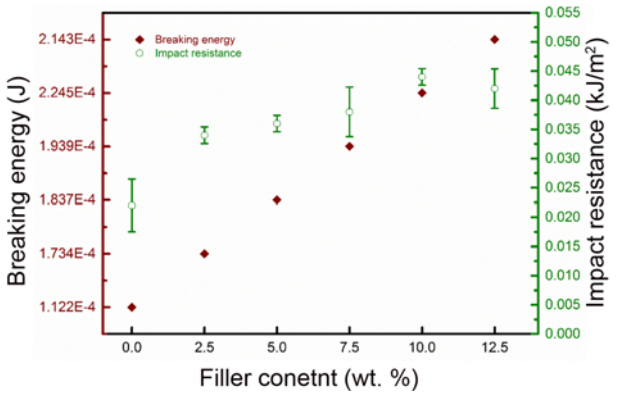

Figure 8. Impact properties vs. filler content.

samples varies from 15 % to 34 % in comparison with the neat epoxy samples whereas same for impact resistance is varied from 14 % to 31 % in the same comparison with the neat polymer. However, after 10 wt. % of filler reinforcement, the impact properties are started to drop for a further reinforcing amount of coir fillers. The associated reason for this mechanism might be connected with the drop in percentage elongation at break for aforesaid composite samples. The radical fall in strain (or elongation) at break has dropped the area under the stress-strain curve, thus consequential fall in breaking energy. The maximum value of breaking energy and impact resistance among all composite samples are found at 10 % of filler weight and the corresponding values are 2.24×10^{-4} J and 0.045 kJ/m^2. The previous research works also showed the comparable properties in terms of impact resistance for different natural filler reinforced plastic materials, which also approves the applicability of the developed coir filler based plastic material. However, the maximum impact resistance found for the present composite material is almost as good as reported for the other reinforced plastic material [45].

Moreover, it should be worth mentioning that this maximum value of impact properties might not be quite sufficient for the certain application, but may be enhanced with the incorporation of impact modifiers. Also, the compatibility between the filler and matrix is a crucial factor for the downfall of mechanical properties, therefore the use of appropriate compatibilizer will also help in improving the impact properties.

The remarkable observations on all the mechanical properties interpreted above signify that the similar variations in different properties can be obtained by including several particle filler loadings and also by changing particle size range. This apprehension might be advantageous for commercial and industrial grade application of this potential lignocellulosic biomass in composite fabrication and attaining the balanced modulus-strength properties without the loss in ecological economics.

Thermo-gravimetric Analysis

The differential thermal analysis (DTA) and weight loss curves of coir filler incorporated epoxy composite samples along with virgin polymer specimens are demonstrated in Figure 9 and 10 for respectively. The DTA curve tells the information about the transformation of materials like glass transitions, crystallization, melting and sublimation during the heating process. It also helps in revealing the information regarding the release and absorbance of heat during dehydration, decarbonation or burning of materials.

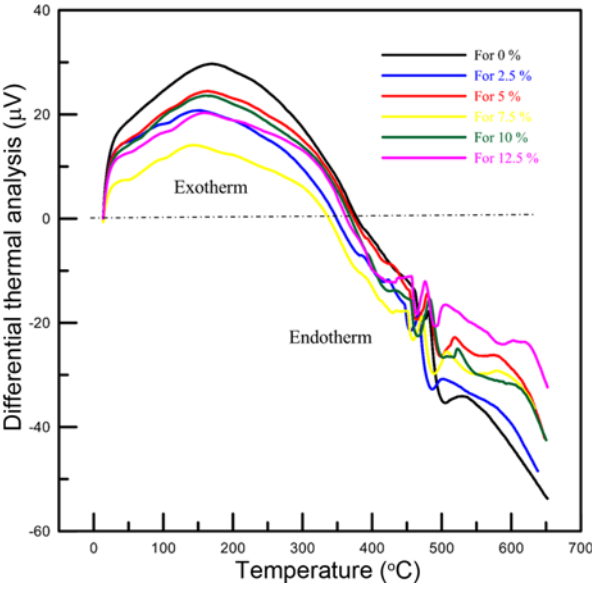

Figure 9. Differential thermal analysis of coir-epoxy composite samples.

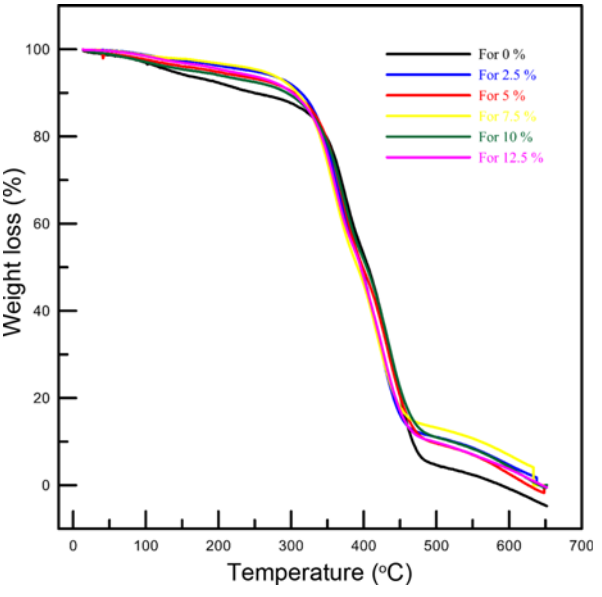

Figure 10. Thermogravimetric analysis of coir-epoxy composite samples.

It can be observed from Figure 9 that the neat epoxy samples (that is 0 % filler content) demonstrated two peaks in the endothermic part of DTA curve, the first one being perceived at 472.8 °C, whereas the second peak at 505.1 °C. Different endothermic peaks correspond to the dehydration and de-polymerization of various constituents. The exothermic part of the curve signifies the cold crystallization in which the sample had been rapidly cooled and frozen into a non-equilibrium state whereas the endothermic part denotes the crystallization melt in a heating run from lower to a higher temperature. The first observed peak might be attributed to the melting of ester groups present in the molecular chain [46] and the second peak is associated with the melting of alkoxide group [47]. The heat absorbed at the first peak is 266.5 mJ whereas the specific energy value for the same is 176.96 J/g. However, at the second endothermic peak, heat absorbed value is increased to 1.70 J and corresponding specific energy to 1.13 kJ/g. The addition of reinforcing material has decreased the observed endothermic peak temperature with the first peak at 468.86 °C and second peak at 499.64 °C for 2.5 wt. % of filler content as shown in Figure 9. The respective values for heat absorbed and specific energy for the first peak are 362.01 mJ and 164.18 J/g while the same for a second peak is 1.03 J and 464.92 J/g. Therefore the heat absorbed is reduced at the second peak for the composite sample as compared to neat epoxy sample. Similar variations are observed for further filler addition from 5 wt. % to 12.5 wt. %. The first endothermic peak for filler content of 5 %, 7.5 %, 10 % and 12.5 % is 467.49 °C, 477.12 °C, 467.36 °C and 475.53 °C respectively. Thus it can be concluded that the behaviour is not much affected by the addition of coir particle fillers to the polymer matrix as two peaks are also depicted for composite samples.

From the practical viewpoint, the thermal stability of any material is associated with the onset of substantial weight loss and can be evidently found in sharp descending inclination in TG curve and designed as onset temperature (T_0). Actually, the onset thermal degradation in natural fibre based composites is a complicated phenomenon owing to the presence of comparative thermal stability of natural fibres and the polymer matrix. Generally, a preliminary loss of weight (<10 %) is perceived below 200 °C and could be due to the water molecules evaporation (moisture, humidity) from filler surface with a minor contribution from synthetic polymer counterparts. Later on increasing the temperature, the depicted weight loss might be due to the non-cellulosic materials like lignin, pectin and waxes. The associated weight loss reflected through the TG curve can be divided into the three stages. The stage I, which resembles the initial weight loss of 10 %, occurs up to about 200 °C. Subsequently, the occurrence of stage II with most of the weight loss (more than 70 %), happens up to about 500 °C. The final or stage III generally encompasses the ending test temperature limit of 800 °C with concluding weight of left-over materials (around 20 %). The presented thermogram curves show that the coir-epoxy composite samples, as well as neat epoxy specimens, exhibited two-step degradation phenomena. The degradation process for the composite along with neat epoxy sample is depicted in Figure 10. The first step of degradation starts at 15 °C and ends at 310 °C. In this process, mass loss is 0.193 mg and 12.815 %. This might be due to the decomposition of light volatiles present in the molecular structure of the epoxy. The second step of degradation starts at 310 °C and ends at 590 °C. The mass loss in this process is 1.308 mg and 86.85 %. In whole, degradation starts 15 °C, ends at 590 °C and total mass loss is 99.668 %. This two-step degradation process continued to happen for the composite sample of 2.5 % filler content as depicted in Figure 10. However, the degradation starts at 28 °C and ends at 310 °C in the first step and the mass loss is 7.48 %. The second step of degradation starts at 310 °C and ends at 650 °C and over 90 % of mass loss occurred in this step. Therefore the whole degradation process starts at 28 °C, ends at 650 °C and the corresponding mass residue at the end of degradation process is 2.16 %. Similar degradation behaviour has been demonstrated for other filler loading samples with some difference in starting and ending temperature along with residue mass. The starting and ending degradation temperature for 5 %, 7.5 %, 10 % and 12.5 % filler samples are 18 °C and 625 °C, 32 °C and 650 °C, 16 °C and 640 °C, 25 °C and 650 °C respectively. The corresponding mass loss for 5 %, 7.5 %, 10 % and 12.5 % filler samples are 99.215 %, 95.602 %, 99.349 % and 99.300 % respectively. The residual mass and onset degradation temperature (T_O) of coir based epoxy composite samples are directly measured from TGA thermograms. The T_O temperature denotes the inflexion point of aforesaid thermogram and the residual mass is the yield left over after heating at 700 °C. Among composite samples, the residual mass is the highest of 7.5 wt. % filler loading owing to the presence of a cluster of coir fillers. The composite samples started to degrade, reached the peak and completed the degradation at a higher temperature with greater residual yield in comparison to neat epoxy specimens. In addition to this, the different conversion took place at a higher temperature for the composite material as compared to neat polymer samples thus indicated the delayed degradation and enhanced thermal stability. Greater thermal stability in case of some coir filler composite sample might be due to the improved interaction of filler with epoxy matrix. In the view of 50 % weight loss temperature, the thermal stability of different coir-epoxy composite samples can be ordered as 7.5 wt. % > 10 wt. % > 2.5 wt. % > 5 wt. % > 12.5 wt. %. Another worth noting point is about the char yield of composite samples. The char yield of coir-epoxy composites is higher than that of the neat epoxy. This divulges the addition of coir particle filler in the epoxy matrix would efficiently advance the char yield which in turn limits the production of combustible gases.

The initial weight loss of the composite samples is associated with the moisture loss and it continued to increase with filler content in the epoxy polymer matrix. Additionally, the higher filler loading brings the thermo oxidative stability in the composite material, thus delaying the maximum weight loss temperature. The inclusion of coir fillers in the polymer matrix significantly improves the char yield, enriches the properties of flame retardancy and oxidation resistance of the material. The thermal onset degradation temperature of composite samples is higher than the same for neat epoxy samples owing to the greater thermal stability of coir fillers [48]. The greater thermal stability for higher filler loading samples is attributed to the better interaction in presence of an improved concentration of coir fillers. The early start of decomposition for most of the composite samples might be connected to the decomposition of pectin and nonstructural hemicellulose as well as the loss of light volatiles from the filler surface. The percentage weight reduction around 650 ^{o}C reflects the amount left at end of degradation of samples. The neat polymer samples have the lowest amount of residue owing to the absence of char. Following this, the composite samples demonstrated the greater amount of residue as compared to the epoxy samples. The depicted thermal behaviour might be helpful in unveiling the budding application of the coir-epoxy plastic material at elevated temperature.

Morphological Observations

The Scanning electron microscopy (SEM) images are utilized in evaluating the filler dispersion in the matrix material in addition to illustrate their fibrillar morphology. The SEM images of composite samples are shown in Figure 11(a), (b), (c) and (d) respectively for 2.5 %, 5 %, 7.5 % and 10 % of filler content.

In Figure 11(a), thin and even dispersion of coir particle fillers can be observed for 2.5 wt. % of filler content. The evenly distributed fillers have proportionately resulted in good load transfer between filler and matrix through the interface and eventually good tensile and flexural properties. As the amount of filler reinforcement is increased, increased filler concentration can be clearly perceived in the Figure 11(b) and (c) for 5 % and 7.5 % of filler weight sample. Further addition of fillers in the epoxy matrix leads to assemblage and cluster formation of filler particles at several places, thus agglomeration of filler clusters and entrapment of resin between them occurs as shown in Figure 11(d). Therefore at this stage, the reinforcement and matrix material found its critical limit and any additional filler content might not serve the desired output as properties enhancement. Hence, for this kind of thermoset matrix, reinforcing weight of filler particles might be good up to 5 to 10 wt. % and further improvement in mechanical properties can be found with the use of compatibilizer to achieve good bonding and better load transfer between the filler and matrix. The impact fracture surfaces of filler reinforced epoxy samples are shown in Figure 12(a) and (b). The impact fracture of filler reinforced composite samples has occurred due to filler debonding.

More precisely, filler debonding and pullout from the polymer matrix can be apparently seen in the presented

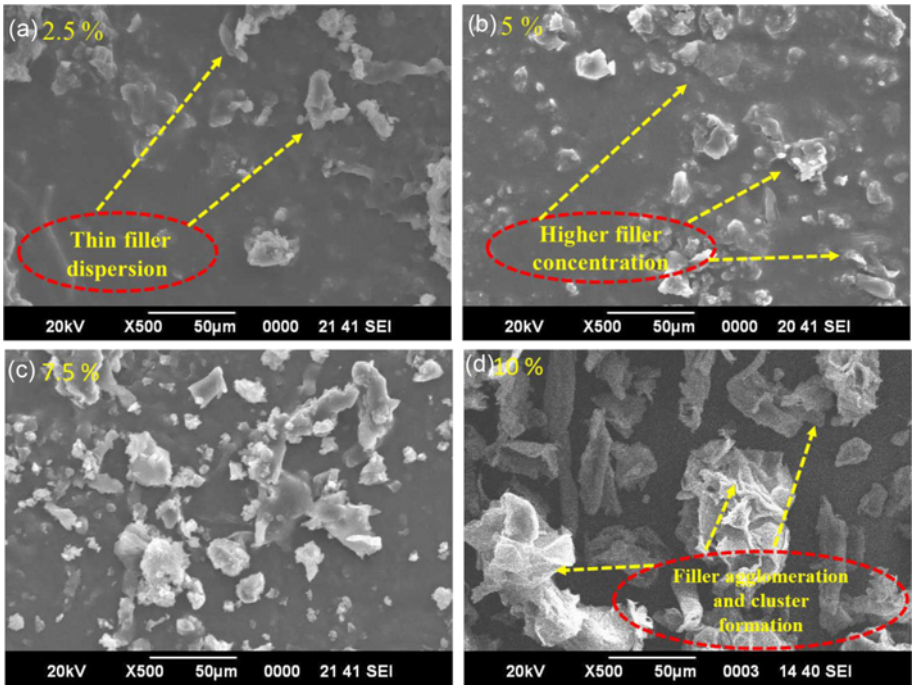

Figure 11. Scanning electron micrographs of (a) 2.5 % (b) 5 % (c) 7.5 %, and (d) 10 % filler content sample.

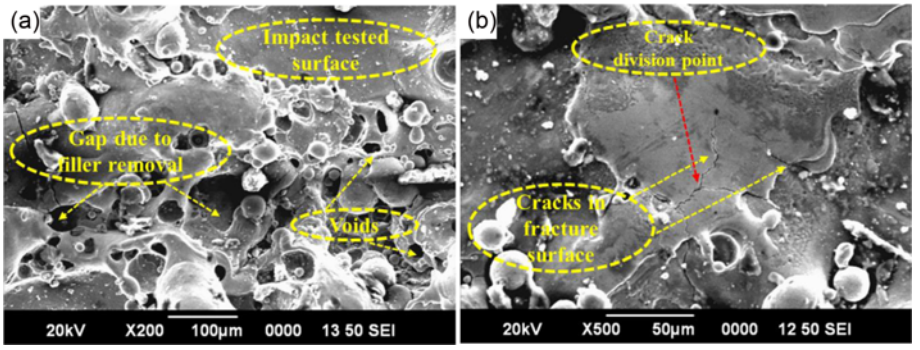

Figure 12. Scanning electron micrographs of impact fracture surface.

fracture surface micrograph. Some cracks are also visible on the surface that could not have propagated fully before the failure happened. The basic fracture mechanism for failure of composite samples is observed to be crack pinning where crack front is pinned at the filler particles encountered point [49]. Moreover, the crack front is then subdivided into two parts as indicated by red arrow in Figure 12(b). This bifurcation of crack propagation line is caused by the presence of coir fillers at the crack tip front. The crack pinning is responsible for enhancing the mechanical properties of filler reinforced composite samples [50].

Concluding Remarks and Future Perspective

The undertaken research work has revealed the potential of coconut coir based particle fillers in form of reinforcement in the thermoset epoxy matrix and demonstrates comparable (or even better) mechanical properties with the existing commercial grade polymer composites. Based on the conducted work, following conclusions can be summarized.

1. The ultimate tensile strength and Young's modulus of the developed composite are found to be maximum and minimum respectively for 2.5 wt. % and 12.5 wt. % of coir filler reinforcement. The maximum value of Young's modulus and tensile strength in case of coir-epoxy composite material are 569 MPa and 22 MPa respectively.
2. The mechanical properties are observed to be influenced by the variation in crosshead speed in such a way that higher crosshead speed resulted in lower tensile strength. Therefore the crosshead speed and filler content play an interdependent role in determining the ultimate properties of composites.
3. The impact resistance and breaking energy of composite samples are found to be significantly improved by coir filler reinforcement. Individual enhancement in impact resistance and breaking energy are by approximately 100 % and 50 % as compared with the neat epoxy sample.
4. The maximum value of fracture toughness and fracture energy is observed for 5 wt. % of filler content and any further addition in filler loading did not materialize in improving the fracture properties. The crack pinning is observed to be the principal mechanism of fracture failure in coir filler reinforced epoxy composite materials.
5. The thermal degradation behaviour is not significantly affected by the filler reinforcement as there is little change in step of degradation. Nevertheless, the starting degradation temperature (T_{Onset}) do affected by the reinforcement like for neat epoxy sample, T_{Onset} is found to be 15 ^{o}C whereas for composite samples, the same varies from 16 ^{o}C to 32 ^{o}C.

Furthermore, the study divulges the prospective use of coir fillers and shows its performance improvement for the epoxy polymer which can establish a value addition process for this important agro-waste in form of product development. In addition, the working temperature of the developed composite material might be around 250 ^{o}C without considerable degradation take place.

A Comment on Material Attributes and Applications

Although the present work has explored the prospective use of coconut coir based particle fillers as reinforcement in the epoxy matrix and investigated the thermo-mechanical properties of the developed bio-based composite material, few potentially interesting observation are its compelling tensile strength, reasonable impact strength and rational mass loss rate. The potential application areas of present material might be electronic casings, furniture (as replacement of timber), decking and fencing.

Acknowledgements

The authors would like to acknowledge CIF-BIT Mesra for providing necessary technical assistances for thermo-gravimetric analysis. The authors also would like to thank Machine element laboratory and Material testing laboratory, MED, NIT Silchar for giving essential research facilities. The first author gratefully acknowledges the Ministry of Human Resource Development (MHRD), GOI for fellowship during his PhD work.

References

1. V. Nagarajan, A. K. Mohanty, and M. Misra, *ACS Sustain Chem. Eng.,* **1**, 325 (2013).
2. M. Arshad, M. Kaur, and A. Ullah, *ACS Sustain Chem. Eng.,* **4**, 1785 (2016).
3. G. Koronis, A. Silva, and M. Fontul, *Compos. Part B Eng.,* **44**, 120 (2013).
4. M. M. Rahman, A. N. Netravali, B. J. Tiimob, and V. K. Rangari, *ACS Sustain Chem. Eng.,* **2**, 2329 (2014).
5. T. T. L. Doan, H. Brodowsky, and E. Mäder, *Compos. Sci. Technol.,* **72**, 1160 (2012).
6. M. Z. Rong, M. Q. Zhang, Y. Liu, G. C. Yang, and H. M. Zeng, *Compos. Sci. Technol.,* **61**, 1437 (2001).
7. L. Yan, N. Chouw, and K. Jayaraman, *Compos. Part B Eng.,* **56**, 296 (2014).
8. N. Saba, M. T. Paridah, and M. Jawaid, *Constr. Build. Mater.,* **76**, 87 (2015).
9. D. V. O. de Moraes, R. Magnabosco, G. H. B. Donato, S. H. P. Bettini, and M. C. Antunes, *Poly. Test.,* **41**, 184 (2015).
10. J. Rencoret, J. Ralph, G. Marques, A. Gutiérrez, A. T. Martínez, and J. C. Del Río, *J. Agric Food Chem.,* **61**, 2334 (2013).
11. L. Yan, N. Chouw, L. Huang, and B. Kasal, *Constr. Build. Mater.,* **112**, 168 (2016).
12. R. B. Yusoff, H. Takagi, and A. N. Nakagaito, *Ind. Crops Prod.,* **94**, 562 (2016).
13. Y. Dong, A. Ghataura, H. Takagi, H. J. Haroosh, A. N. Nakagaito, and K. T. Lau, *Compos. Part A Appl. Sci. Manuf.,* **63**, 76 (2014).
14. J. Sarki, S. B. Hassan, V. S. Aigbodion, and J. E. Oghenevweta, *J. Alloys. Compd.,* **509**, 2381 (2011).
15. J. Kalibová, L. Jačka, and J. Petrů, *Solid Ear.,* **7**, 469 (2016).
16. U. J. Etim, S. A. Umoren, and U. M. Eduok, *J. Saudi Chem. Soc.,* **20**, S67 (2016).
17. B. Ramaraj, *Polym. Plast. Technol. Eng*., **45**, 1227 (2006).
18. J. Cho, M. S. Joshi, and C. T. Sun, *Compos. Sci. Technol*., **66**, 1941 (2006).
19. A. Zykova, P. Pantyukhov, and A. Popov, *Polym. Eng. Sci.,* **57**, 756 (2017).
20. V. Nagarajan, A. K. Mohanty, and M. Misra, *ACS Omega,* **1**, 636 (2016).
21. W. Wang and G. Huang, *Mater. Des.,* **30**, 2741 (2009).
22. M. G. Roudsari, A. K. Mohanty, and M. Misra, *ACS Sustain. Chem. Eng.,* **5**, 9528 (2017).
23. S. M. Sapuan, M. Harimiand, and M. A. Maleque, *Arab. J. Sci. Eng*., **28**, 171 (2003).
24. R. Kumar, S. Bhowmik, and K. Kumar, *Int. Polym. Proc.,* **32**, 308 (2017).
25. P. Kumar, D. M. Barrett, M. J. Delwiche, and P. Stroeve, *Indus. Eng. Chem. Res.,* **48**, 3713 (2009).
26. M. M. Haque, M. E. Ali, M. Hasan, M. N. Islam, and H. Kim, *Indus. Eng. Chem. Res.,* **51**, 3958 (2012).
27. R. Narendar, K. P. Dasan, and S. Kalainathan, *Poly. Comp.,* **38**, 1671 (2017).
28. S. Jayabal, S. Velumani, P. Navaneethakrishnan, and K. Palanikumar, *Fiber. Polym.,* **14**, 1505 (2013).
29. M. Hudspeth, X. Nie, W. Chen, and R. Lewis, *Biomacromolecules*, **13**, 2240 (2012).
30. K. J. Wong, B. F. Yousif, K. O. Low, Y. Ng, and S. L. Tan, *J. Strain. Anal. Eng. Des*., **45**, 67 (2010).
31. R. Kumar, K. Kumar, P. Sahoo, and S. Bhowmik, *Proce. Mater. Sci.,* **6**, 551 (2014).
32. N. M. Abdullah and I. Ahmad, *Fiber. Polym.,* **14**, 584 (2013).
33. J. T. Kim and A. N. Netravali, *J. Agric. Food. Chem*., **58**, 5400 (2010).
34. C. Diao, T. Dowding, S. Hemsri, and R. S. Parnas, *Compos. Part A Appl. Sci. Manuf.,* **58**, 90 (2014).
35. A. K. Balan, S. M. Parambil, S. Vakyath, J. T. Velayudhan, S. Naduparambath, and P. Etathil, *J. Mater. Sci.,* **52**, 6712 (2017).
36. R. Kumar, K. Kumar, and S. Bhowmik, *Wood Sci. Technol.,* **52**, 677 (2018).
37. C. K. Seong, S. Husseinsyah, and F. N. Azizi, *Polym. Plast. Technol. Eng*., **52**, 287 (2013).
38. F. Z. Arrakhiz, E. M. Achaby, A. C. Kakou, S. Vaudreuil, K. Benmoussa, R. Bouhfid, O. Fassi-Fehri, and A. Qaiss, *Mater. Des.,* **37**, 379 (2012).
39. M. N. Islam, M. R. Rahman, M. M. Haque, and M. M. Huque, *Compos. Part A Appl. Sci. Manuf.,* **41**, 192 (2010).
40. A. D. Cavdar, F. Mengeloğlu, and K. Karakus, *Measurement*, **60**, 6 (2015).
41. R. Kumar, K. Kumar, and S. Bhowmik, *J. Polym. Environ.,* **26**, 2522 (2017).
42. T. H. Ly, J. Zhao, M. O. Cichocka, L. J. Li, and Y. H. Lee, *Nat. Commun*., **8**, 14116 (2017).
43. S. Yang, V. B. Chalivendra, and Y. K. Kim, *Compos. Struct.,* **168**, 120 (2017).
44. A. Shekhawat and R. O. Ritchie, *Nat. Commun.,* **7**, 10546 (2016).
45. K. Gokul, T. R. Prabhu, and T. Rajasekaran, *Trans. Ind. Inst. Metals,* **70**, 2537 (2017).
46. L. Bouzidi, S. Li, D. S. Biase, S. Q. Rizvi, and S. S. Narine, *Ind. Eng. Chem. Res.,* **52**, 2740 (2013).
47. M. Nakano, T. Wada, and N. Koga, *The J. Phys. Chem. A*, **119**, 9761 (2015).
48. A. C. Milanese, M. O. H. Cioffi, and H. J. C. Voorwald, *Compos. Part B Eng.,* **43**, 2843 (2012).
49. R. Kitey, A. V. Phan, H. V. Tippur, and T. Kaplan, *Int. J. Fract.,* **141**, 11 (2006).
50. S. Biswas, S. Kindo, and A. Patnaik, *Fiber. Polym.,* **12**, 73 (2011).